Globally coupled chaotic maps and demographic stochasticity

David A. Kessler* and Nadav M. Shnerb†
Department of Physics, Bar-Ilan University, Ramat-Gan 52900 Israel

The effect of noise on a system of globally coupled chaotic maps is considered. Demographic stochasticity is studied since it provides both noise and a natural definition for extinction. A two-step model is presented, where the intra-patch chaotic dynamics is followed by a migration step with global dispersal. The addition of noise to the already chaotic system is shown to dramatically change its behavior. The level of migration in which the system attains maximal sustainability is identified. This determines the optimal way to manipulate a fragmented habitat in order to conserve endangered species. The quasi-deterministic dynamics that appears in the large N limit of the stochastic system is analyzed. In the clustering phase the infinite degeneracy of deterministic solutions emerges from the single steady state of of the stochastic system via a novel mechanism that involves an almost defective Markov matrix.

PACS numbers: 87.23.Cc , 64.70.qj, 05.45.Xt, 05.45.-a

INTRODUCTION

The dynamics of coupled chaotic maps has attracted a lot of interest in the last two decades, following the pioneering works of Kaneko [1, 2]. A substantial part of the study is focused around the paradigmatic model of globally coupled maps, where many fundamental results such as mutual synchronization, dynamical clustering and glassy behavior were demonstrated [3, 4]. The universal character of the chaotic dynamics makes the coupled maps model relevant to many phenomena, ranging from neural systems and human body rhythms to coupled lasers and cryptography [3, 4].

If the coupling between subsystems is diffusive, the whole system admits an invariant manifold where the chaotic motion is fully synchronized and all patches are in the same state at the same time. There are no density gradients and the diffusive coupling has no role. The stability of this invariant manifold depends on the relative strength of the diffusion (that tends to suppress local fluctuations and so stabilize the coherent state) with respect to the exponential divergence of nearby trajectories within the chaotic attractor.

A diffusive globally coupled system is thus characterized by these two parameters: the diffusion among patches and the strength of the chaotic separation (usually quantified by the Lyapunov exponent of the attractor) [3, 5]. In the weak diffusion, strong chaotic separation regime the coupling among patches is negligible and any given subsystem moves independently on the chaotic attractor with almost no correlation between different patches; this is the turbulent phase. In the opposite limit of weak chaos and strong migration the whole system is fully synchronized as the invariant manifold becomes a global attractor. Between these two extremes lies the clustering phase, where the system segregates spontaneously into a few groups of patches with all subsystems in the same group fully synchronized.

This problem of coupled chaotic maps emerges naturally while considering spatially extended ecologies (metapopulations) [6]. The population dynamics of a large, well-mixed system is often modeled by a single chaotic map like the logistic [7] and the Ricker [8] maps. If instead of being well-mixed, the population is divided into a number of sub-populations connected by migration, one arrives at the coupled map problem. It should be noted, however, that the numbers of individuals on each habitat patch are often relatively small. The system is thus affected by intrinsic stochasticity associated with the discreteness of animals; the number of individuals on certain patch is an integer that differs from the predictions of the deterministic theory. This *demographic stochasticity* (shot noise) always exists, even in the absence of external noise. In particular, the logistic map and the Ricker map, in their chaotic phases, visit states for which the population density is arbitrary close to zero. While the deterministic dynamics predicts a recovery of the system, the fact that the population is made of individuals means that very small densities actually correspond to total *extinction*. The discreteness of individual agent, thus, plays a double role: it introduces stochasticity into the dynamics and it allows for local and global extinctions.

A population of discrete agents that obeys these types of chaotic dynamics is extinction-prone. A sustainable community appears only due to the rescue effect [9], i.e., due to recolonization of empty patches by individuals that immigrate from other habitat patches. While it is quite hard to test this conjecture in field studies, many old [10–12] and recent [13–16] lab experiments suggest that the well-mixed dynamics of simple ecosystems (single species or victim-exploiter systems) are indeed extinction prone, and that the system acquires stability only due to its spatial structure, a result supported also by numerical simulations of many models [17–20]. These experiments show that the system acquires the state of maximum sustainability for *intermediate* levels of migration. If the diffusion is too weak local extinctions ac-

cumulate to yield a global one, so the lifetime of the whole population grows with diffusion. On the other hand strong diffusion is also harmful as it leads to full [5] or intermittent [21] synchronization that allows for correlated extinction.

One of the central practical issues that emerges from this insight is known as the "conservation corridors" problem [5, 21, 22]. Trying to protect endangered species and to reduce the effect of habitat fragmentation, habitat corridors have been proposed as a means of increasing movement between patches, thus allowing rescue of locally extinct colonies. Corridors, however, have become controversial due to the realization that they can synchronize the dynamics of different patches and expose the system to the danger of correlated global extinction. The chance of global extinction is very sensitive to the total size of the population. Accordingly, the onset of a drought or a new infectious pathogen poses a much higher threat to the continued existence of the species, if the internal dynamics has brought the total population to a temporal minimum.

The role of a conservation biologist is to design the corridors so as to ensure optimal sustainability of the whole system, which obtains when the minimum over time of the total population is maximal [23]. This task is performed using models that take into account a few basic, measurable parameters of the system, like the maximum fecundity r, the carrying capacity N and the rate of dispersal ν (see concrete examples in [5, 22]).

The theoretical work done so far in that field assumed noise-free deterministic dynamics. It was focused on the conditions under which coherence among patches [5, 21] may appear, and on the identification of the clustering phase [24, 25] where attractive orbits of the deterministic dynamics emerges. Beyond this deterministic approach lies the assumption that stochasticity induces only small fluctuations around the deterministic trajectories and, in particular, affects only weakly the stability of the attractive orbits. In a recent work [26] it was found that for small spatial systems the stable manifold is excitable and allows for long transients once the system is kicked out its narrow basin of attraction. Here, we examine this effect in a fully coupled system, showing that reasonable levels of noise alter substantially the dynamics expected from the deterministic theory.

The aim of this paper is twofold. First there is a practical issue: we show how to identify the *maximum sustainability point* given the basic parameters of the system. This point appears in the dynamical clustering phase, where the deterministic theory predicts an infinite set of stable solutions [3]. It turns out that demographic stochasticity lifts this degeneracy and so yields a single dynamical solution for each set of parameters, thus providing us with an unambiguous criteria for optimal resilience against exogenous environmental perturbations.

Our second, more abstract, goal is to explore the "semideterministic" limit, i.e, to understand how the results of the deterministic theory are retrieved in the limit of no stochasticity. The strength of demographic stochasticity is inversely proportional to the square root of the typical number of individuals N on each patch, and the noise vanishes in the $N \to \infty$ limit. In particular one may ask how the infinite degeneracy that characterizes the clustering phase in the deterministic model is retrieved in the large N limit of the stochastic theory.

Throughout this paper we restrict ourselves to demographic stochasticity since it allows for a natural definition of extinction as the "absorbing state" where the number of animals is zero and the dynamics halts. The qualitative results, however, hold for other types of noise as well.

THE STOCHASTIC-CHAOTIC COUPLED MAP

Let us present first the deterministic dynamics of a globally coupled chaotic population [1–4]

$$s_{t+1}^i = (1-\nu)F(s_t^i) + \frac{\nu}{L}\sum_{j\neq i} F(s_t^j). \qquad (1)$$

Here, s_i is the a measure of the population density on the i-th site and F is the chaotic map. ν is the migration parameter (the chance of an individual agent to leave its site) and $1 \leq i \leq L$, where L is the number of patches. The paradigmatic model (1) is exact only in the zero noise limit, e.g., when the population on each patch is large enough so that the relative fluctuations associated with demographic stochasticity vanish.

To begin our discussion we specify a stochastic model. We have, as in the deterministic models, a collection of L sites, where the local population density s_i is now replaced by an integer n_i. The update proceeds in two steps. First, the reproduction and competition generate a new value of n_i. This value is taken to be drawn from a Poisson distribution with mean $F(n_i)$, where $F(n)$ is, as before, the chaotic map. In this paper, we take as our choice of F the well-known Ricker map [8], $F(n) = rne^{-n/N}$, with maximum fecundity $r = 20$ well in the chaotic regime. (The Ricker dynamics has been chosen just because it simplifies our numerics; our results hold for a broad range of different maps, and we believe that any extinction-prone chaotic map should exhibit similar behavior. In particular, we have verified that the logistic map (when defined as zero outside the range $0 \leq s_i \leq 1$) yields qualitatively similar results.) The second step is dispersal, in which with probability ν, each of the inhabitants of every site can decide to leave and pick a new site at random. This model is essentially similar to that used by Hamilton and May [27] to study optimal dispersal rates, except for the chaotic nature of the on-site reproduction/competition dynamics of the present model.

For the sake of concreteness one may think about a population of butterflies spatially segregated among L habitat patches, with n_i individuals on the ith patch. Before the cold season each individual deposit r eggs, but the chance of the caterpillar to survive and become an adult butterfly is $exp(-n_i/N)$ (the chance is much smaller on crowded habitat patches due to competition). This is the reproduction-competition step. A fully developed adult may then leave its natal community (during the "migration step") with probability ν and immigrate (with equal chance) to any other habitat patch, where it will deposit its eggs for the next year [28].

We have simulated this system directly using Monte-Carlo technique for L's up to 10000. However for the purpose of analysis, it is more convenient to study, as do Hamilton and May, the $L \to \infty$ limit. This limit is completely characterized by a probability distribution ψ_n^t, the chance of a given site to have n individuals at time t.

For any habitat patch the stochastic reproduction-competition step is fully specified by a Markov matrix Q^1, where Q^1_{mn} is the chance of n butterflies that deposit eggs on that island to produce m adult butterflies in the next spring. Q^1 is the same for all patches and depend solely on the details of the chaotic map F. The migration step is described by another Markov matrix Q^2, for which the (k, m) entry is the chance to have k residents on a patch after the migration step if there were m before. Clearly this matrix depends not only on the chance of migration ν but also on the average population per island before the migration step.

The dynamics described by Eq. (1) may thus be replaced by a Master Equation for ψ_n^t, with the Markov matrix $\mathcal{M} = Q^2 Q^1$. This can be shown to reduce to

$$\psi_n^{t+1} = \sum_{m=0}^{\infty} \psi_m^t e^{-\mu(m)} \frac{\mu(m)^n}{n!} = \mathcal{M}_{nm} \psi_m^t \qquad (2)$$

where $\mu(m) = F(m)(1-\nu) + \nu\lambda$ is the expected number of individuals who will occupy a site that started with m individuals and λ is the mean number of offspring (that reached adulthood) per site, given by

$$\lambda = \overline{F(m)} = \sum_{m=0}^{\infty} \psi_m F(m). \qquad (3)$$

The update rule, which involves multiplying the probability vector ψ by the transformation matrix $\mathcal{M}$, is, despite appearances, nonlinear, as $\mathcal{M}$ depends nonlinearly on the parameter λ which itself depends on the input state. The update rule preserves probability, as it must, since for any given λ it has the Markov property.

TO THE SYNCHRONIZED PHASE VIA PERIOD DOUBLING CASCADE

To get an overview of the dynamics of our system, we consider a relatively small $N = 5$, and integrate the system forward in time using the Master equation described above. Since the state space is in principle infinite, we truncate all states with more than $10N$ individuals on a site. Due to the exponentially falloff of the Ricker map, this truncation is completely harmless. For very small ν, we find that the average number of individuals per site falls exponentially in time, with the percentage of extinct sites exponentially approaching unity. This is as expected, since there is a finite probability for an individual site to go extinct and without sufficient dispersal to enable recolonization, more and more sites go extinct as time goes on. The system cannot go completely extinct because we are simulating the $L = \infty$ limit. With a finite number of sites, the system would indeed go extinct. This is the scenario conservation ecologists are trying to avoid by constructing corridors and thereby increasing ν.

Increasing ν beyond some critical value, the system now settles into a unique nontrivial time-independent state, independent of initial conditions. The average occupancy increases with increasing ν, until another bifurcation is encountered, at which point the system goes into a period-two state. This state is also independent of initial conditions. This period-two bifurcation is then followed at yet larger ν by a period-4 bifurcation. Eventually beyond some ν the system exhibits chaotic behavior. This course of events is summarized in the top panel of Fig. 1.

We start our analysis be considering the constant (period 1) solution, which is a solution of the nonlinear equation

$$\mathcal{M}(\lambda[\psi])\psi = \psi \qquad (4)$$

Finding a solution is rendered much more tractable by breaking the equation into two simultaneous equations:

$$\begin{aligned} \mathcal{M}(\lambda)\psi &= \psi \\ \lambda &= \sum_{m=0}^{\infty} \psi_m F(m). \end{aligned} \qquad (5)$$

In the first of the these equations, λ is an *arbitrary* parameter, which has to satisfy the auxiliary second equation. Solving the first of these two equations is straightforward, as it is now linear. For any given value of λ, the matrix $\mathcal{M}(\lambda)$ admits, due to the Markov property, a unique invariant eigenvector $\psi_* = \psi_*(\lambda)$ (i.e., a right eigenvector with eigenvalue unity). However, for general λ, the second equation is violated. We can define a "mismatch function"

$$g(\lambda) \equiv \lambda - \sum_{m=0}^{\infty} [\psi_*(\lambda)]_m F(m) \qquad (6)$$

It is now a simple matter to scan in λ and locate the zero crossings of g. In general there are two such zeros, one at $\lambda = 0$, in which case $(\psi_*)_m = \delta_{m,0}$ as well as one at positive λ. However, for small enough ν, the first of these, which represents the absorbing state, is in fact the *only* period-one solution. This is consistent with the simulation above, where the system for small ν converged exponentially to the absorbing state. The range of ν's for which the only stationary state is the absorbing state decreases rapidly with N, since local extinctions become rarer at large N.

Above the critical ν, as noted above, a second, non-trivial period-one solution emerges. The figure shows the average occupancy $\overline{n}(\nu)$, which rises from zero at the critical ν, reaches a maximum and then slightly decreases for larger ν. A sample distribution for this period-one solution is shown in Fig. 2, and is characterized by having two peaks, each having half the probability. The system thus decomposes into two clusters that oscillate 180° out of phase with respect to the other. Since the two clusters have equal weight, the overall occupancy of the system is time-independent.

The period-one solution was seen in simulation to go unstable at the point of maximal occupancy, bifurcating to a period-two solution. These period-2 solutions may be constructed using a similar strategy as that described above for the period one solution. Picking arbitrary values for λ_1 and λ_2 the Markov matrix $\mathcal{M}(\lambda_2)\mathcal{M}(\lambda_1)$ must admit an invariant eigenvector $(\psi_*)_m$. The solution is consistent *iff* the system satisfies the two auxiliary conditions $\lambda_1 = \sum(\psi_*)_m F(m)$ and $\lambda_2 = \sum \left[\mathcal{M}(\lambda_1)(\psi_*)\right]_n \; F(n)$. Extending this procedure one may find orbits of higher periodicity by searching through the space of quartets and octets of λ's with the appropriate auxiliary conditions.

This succession of bifurcations presumably recapitulates the standard period-doubling route to chaos. One can prove in fact that the system is indeed chaotic as $\nu \to 1$. As pointed out by Durrett and Levin [17], in that case the occupation of a site just before the reaction step is a Poisson distribution with a mean given by the total population in the last step. As a result, $\overline{n}$ satisfies the iterative map,

$$\overline{n}_{t+1} = \sum_k kF(k)e^{-\overline{n}_t}\frac{(\overline{n}_t)^k}{k!} \qquad (7)$$

where F is the deterministic map. In the Ricker case the resulting map for $\overline{n}$ is also unimodal and the resulting transformation is chaotic in the regime of parameters considered here. This also implies that any periodic orbit must lose its stability as ν approaches unity.

The general scheme that emerges for strong stochasticity from the upper panel of Fig. 1 and from Fig. 2 should be compared with the results of the deterministic theory based on Eq. (1). The deterministic system

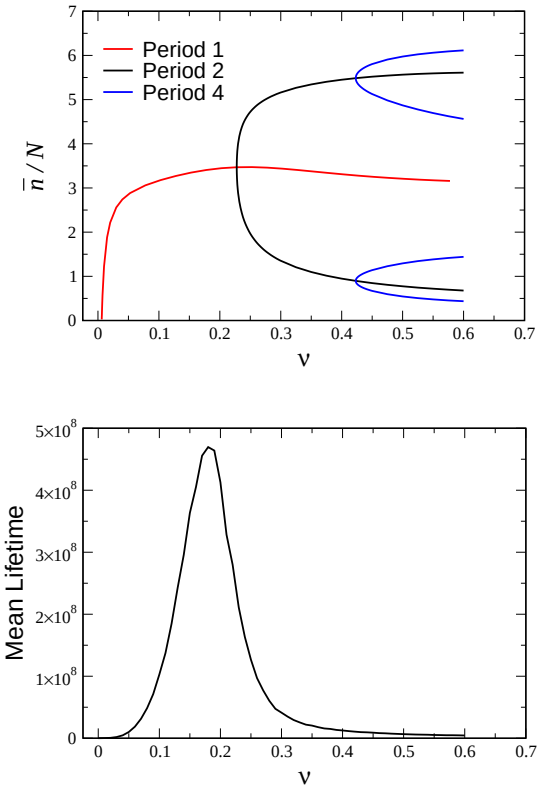

FIG. 1: Upper: Solution branches for $N = 5$, showing the period 1, 2 and 4 branches as a function of ν. Lower: Mean lifetime of a system of fives sites as a function of ν for $N = 5$. As explained in the main text, maximal sustainability is achieved on the edge of the first bifurcation.

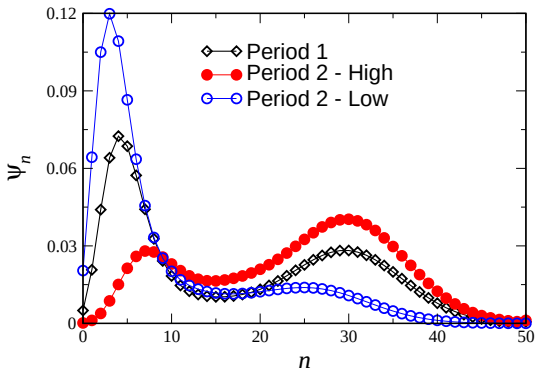

FIG. 2: Probability Distributions ψ_n for the period 1 solution at $\nu = 0.2$ and for the two phases of the period 2 solution at $\nu = 0.25$. The points are connected to guide the eye.

admits a synchronized chaotic phase at large ν, a turbulent phase at small ν and a clustering phase in between. In its broad outlines, this structure is preserved in the stochastic theory. At large ν in both theories the average occupancy of the system behaves chaotically. At intermediate ν, the system in both cases exhibits small period oscillations characteristic of clustering. However, there are major differences between the two cases.

1. In the clustering phase, there are many stable attractors in the deterministic case, and the particular attractor the system chooses is a function of the initial conditions. With strong stochasticity (small carrying capacity N) we find that the infinite degeneracy of the deterministic clustering phase has been eliminated; there is only one stable solution for a given ν.

2. The broad distributions shown in Fig. 2 replace the delta peaks of of the deterministic theory [3].

3. The transition to chaos through a cascade of period-doubling bifurcations is also absent in the deterministic system.

4. Both theories exhibit a phase with constant average occupancy at smaller ν. However, the nature of this phase differs between the two cases. In the deterministic theory, the constant output of the entire system is the result of a complete lack of coordination between the behavior at different sites. In the stochastic theory, at least close to the onset of the period-2 solution, the behavior is more aptly characterized as a symmetric two-cluster phase. Such symmetric solutions are also present in the deterministic system, but have to compete with the much more numerous asymmetric two-cluster solutions, with their period-2 behavior.

5. At smaller ν in the deterministic system there is a sharp transition to completely unsynchronized (turbulent) behavior, whereas in the strongly stochastic system there is a smooth widening of the occupancy distribution. Also, here the correlation time of the spatial pattern decreases continuously until the extinction transition.

6. Clearly the extinction phase is a consequence of turbulence. However, the transition from the turbulent phase to the cluster phase in the deterministic system occurs at much higher ν than the extinction transition for the stochastic system (which is exponentially small in N, and quite small even for $N = 5$).

MAXIMAL SUSTAINABILITY

Returning to the practical problem of conservation corridors, what the ecologist really wants is to identify the maximum sustainability point, i.e., under what conditions the average time to extinction of the endangered species will be maximal. Our results suggest a simple answer: the conservative engineer should try to construct the corridors such that ν corresponds to *the edge of the bifurcation from period one to period two.* At this point the system supports the highest constant population. Above this value there are low-population periods (years, seasons) in which the chance of correlated extinction due to global catastrophe is much higher. We can see this directly by looking at a small L, small N system, which is in any case the most relevant in the ecological context [5, 21]. Even in the presence of an attractive manifold such a small system will sooner or later go extinct as a result of demographic fluctuations.

We have used Monte-Carlo simulation to measure the mean time to extinction as a function of ν; results are shown in the lower panel of Fig. 1. There is a sharp peak right where we expect, just before the bifurcation to the period-2 solution. This feature is even more pronounced in the presence of environmental noise, but the exact results are of course sensitive to the strength of the noise and the exact form of the coupling of the noise to the dynamics.

THE DETERMINISTIC (LARGE N) LIMIT

As in other fields of science, from quantum-classical correspondence to the theory of reaction kinetics, the deterministic description of a system should be understood as the limit in which the underlying stochastic fluctuations may be neglected. For the system considered here this corresponds to the $N \to \infty$ limit. In this limit the extinction region shrinks to zero, there is a sharp distinction between the turbulent and the clustering phase, and the clustering phase itself exhibits degeneracy, i.e., many solutions exist for the same set of parameters [3]. Our numerics is limited by the size of the Markov matrices and currently we can find solutions for N up to 80 (beyond that we must use the MC technique). The nature of the large N limit has to be analyzed separately in the various phases of the deterministic theory. Here we wish to discuss in detail just the behavior in the clustering phase, where the restoration of degeneracy occurs in a novel fashion; namely, by the appearance of a near degeneracy (defectiveness) of the Markov matrix.

The clustering phase

To begin our numerical investigation, let us start to increase N. For $N = 10$ (results not shown) the bifurcation from period 1 to period 2 is backward (subcritical), while the bifurcation from period 2 to period 4 is still forward even at $N = 20$. The location of the bifurcation from period 1 to 2 is almost independent of N, but the bifurcation from 2 to 4 is strongly N dependent, moving to smaller ν as N increases. In fact, by $N = 40$ it has already moved to the backward branch of the period 2 solution. This situation is presented in the upper panel of Fig. , where the period 1, 2 and 4 solution branches are traced out for $N = 60$.

The most important issue here is how the deterministic continuum of period two solutions is recovered as N grows to infinity. As explained above, the period 2 solutions are identified by searching for all pairs of λ_1, λ_2 that admit an invariant eigenvector ψ such that $\lambda_1 = \sum \psi_n F(n)$, and $\lambda_2 = \sum F(n) \left[\mathcal{M}(\lambda_1)\psi\right]_n$. It turns out that, for large N, there is a range of λ_1, λ_2 for which the Markov matrix $\mathcal{M}_{21} \equiv \mathcal{M}(\lambda_2)\mathcal{M}(\lambda_1)$ admits, in addition to its invariant eigenvector, an eigenstate $\tilde{\psi}$ with an eigenvalue very close to 1, say, $1 - \epsilon$. Thus, up to a small term (for $N = 80$, e.g., $\epsilon = 10^{-12}$) any linear combination of the first and the second eigenvectors imitates the real invariant state until $t \sim 1/\epsilon$. Within this time horizon one has, effectively, a *continuous family* of invariant eigenvectors of $\mathcal{M}_{21}$, $\alpha\psi + (1-\alpha)\tilde{\psi}$. The two auxiliary conditions no longer are sufficient to determine a solution. We call these solutions for which we ignore ϵ a *quasi-solution*, of which there exists a continuous family depending on α. It turns out that ϵ decreases sharply with increasing N; the deterministic limit emerges from this continuous family of solutions as explained below.

In Fig. 4, we see all this exemplified in a simulation, where we plotted $\overline{n}_t$ as a function of t, for $N = 60$, $\nu = 0.21$. We see that for times less than roughly $5 \cdot 10^5$, the system exhibits an essentially period 2 type behavior, with an extremely slow drift of the two states. Suddenly, beyond this point, the system converts to a period 4 behavior. A good way of analyzing the drift is to plot $\overline{n}_{2t+1}$ vs. $\overline{n}_{2t}$, as seen in Fig. (lower panel). If the system had a true period 2 orbit, this graph would show a single point. Instead, the drift converts this into a curve. The points on this curve coincide precisely with the above described quasi-solutions, a number of which are indicated by circles. The true solutions are represented by triangles (period 2) and a diamond (period 1) in the figure. The system drifts to larger amplitude oscillations, until the instability is encountered and it goes to a period 4 orbit, represented by two dots in the figure. While there are quasi-solutions (as well as a true solution $\alpha = 0$) beyond this point, they are not dynamically relevant due to their strong instability.

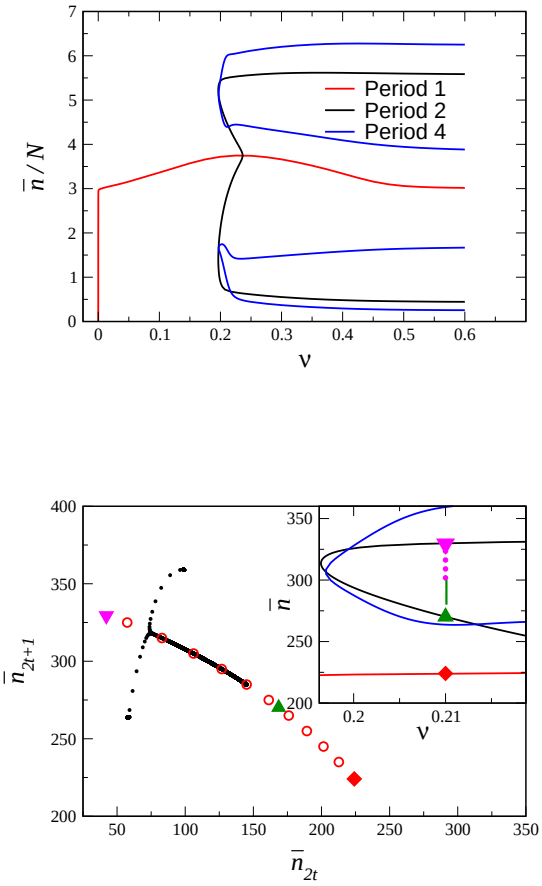

FIG. 3: Upper: Solution branches for $N = 60$, showing the period 1, 2 and 4 branches as a function of ν. Lower: The return map $\overline{n}_{2t+1}$ versus $\overline{n}_{2t}$, indicated by black dots, for $N = 60$, $\nu = 0.21$, taken from the simulation depicted in Fig. 4. The trajectory - a drift away from the green triangle, up to the point it splits to the period 4 orbit - is determined by the line of quasi solutions indicated by the red circles. The triangles represent true period 2 solutions for which $\alpha = 0$, and the period 1 solution is indicated by a red diamond. The inset is a blowup of the relevant section of the upper panel, indicating the true solutions and the slow flow through the quasi-solutions. The solutions for $\nu = 0.21$ are marked by the same symbols as in the main figure. For these parameters the dynamics close to the green triangle is so slow that measuring the dynamics becomes impractical. When $N \to \infty$, all the region between the green triangle and the splitting point (indicated by full green line in the inset) becomes marginally stable.

The turbulent phase

The above picture of the large N limit of the clustering phase is very different than that which obtains for small ν, where the deterministic theory is in the turbulent phase. This aspect of the problem has been already considered by Shibata, Chawanya and Kaneko [29]. These authors studied numerically the system described by Eq. (1) with the logistic map and additive noise. [as explained above there is no essential difference between

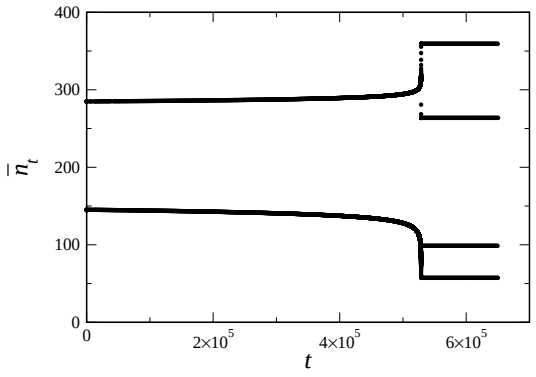

FIG. 4: The average population $\overline{n}_t$ versus t for $N = 60$, $\nu = 0.21$. Data obtained by direct integration of the Master equation, Eq. (2).

demographic stochasticity and other types of noise, including additive noise, as long as the system is far from the extinction state]. They restricted themselves to very small noise, so that the system would not blow up (which happens if the logistic map is not defined as zero for arguments outside the range 0 to 1). They discovered that for these very small noises the system is governed by a relatively low-dimensional attractor. They further found that the dimensionality of this attractor increases as the noise gets smaller, and in this way the turbulent phase is recovered. We were able to reproduce the results of [29] in our demographic stochasticity system using the MC technique with $N = 10^6$ and above. For smaller N, i.e,. larger noise, the system is in the period-one state we have described above.

While more work is needed to fully characterize the transition to turbulence, the evidence so far suggests the following scenario: As N increases the period 1 solution at small ν undergoes a Hopf-like bifurcation to some low-dimensional chaotic attractor and then the dimensionality of this attractor increases with N to yield turbulence. The critical N for this bifurcation appears to be very sensitive to ν, and in particular grows dramatically as ν decreases.

The synchronized phase

More work is also necessary to fully characterize the large-N behavior of the synchronized phase. In particular, the deterministic system is known to exhibit intermittency when ν is slightly below the transition to synchronous behavior [21]. It is interesting to consider how this tendency to intermittency manifests itself for large finite N. Preliminary work indicates that the variance of the occupancy exhibits sharp bursts in this regime, but the details have yet to be worked out.

In summary, then, we have seen that adding demographic noise to a globally coupled chaotic map has a marked effect on the dynamics, leading in fact to very regular dynamics for intermediate coupling strength. The stochastic system supports a well defined stable orbit in the clustering phase, this allows one to identify the point of maximum sustainability. As the noise strength is reduced, the clustering phase exhibits an exponentially long time scale, which effectively gives rise to the continuous family of solutions seen in the no-noise limit.

We wish to thank K. Kaneko for useful comments on a previous version of the manuscript. NMS thanks EU 6 framework CO3 pathfinder for support.

* Electronic address: kessler@dave.ph.biu.ac.il
† Electronic address: shnerbn@mail.biu.ac.il

[1] K. Kaneko, Phys. Rev. Lett. **63**, 219 (1989); Physica **D 41**, 137 (1990).
[2] K. Kaneko, I. Tsuda, Complex systems: Chaos and Beyond (Springer-Verlag, Berlin Heidelberg 2001).
[3] See a summary in: S.C. Manrubia, A.S. Mikhailov, and D.H. Zanette, *Emergence of Dynamical Order: Synchronization Phenomena in Complex Systems* (World Scientific, Singapore, 2004).
[4] For general reviews see *Theory and Applications of Coupled Map Lattices*, edited by K. Kaneko (Wiley, New York, 1993); A. Pikovsky, M. Rosenblum, and J. Kurths, Synchronization: A Universal Concept in Nonlinear Sciences, (CUP, Cambridge, 2001); S. Boccaletti, V. Latora, Y.Moreno, M. Chaves, and D.-U. Hwang, Physics Reports **424**, 175 2006.
[5] D.J.D. Earn, S.A. Levin and P. Rohani, *Science* **290**, 1360 (2000); D.J.D. Earn and S.A. Levin, PNAS **103**, 3968 (2006).
[6] I. A. Hanski and M.E. Gilpin, *Metapopulation Biology: Ecology, Genetic and Evolution* (Academic Press, San Diego 1997).
[7] R. M. May, Nature **261**, 459 (1976).
[8] W. E. Ricker, J. Fisheries Res. Board Can., **11** 559, 1954.
[9] J. H. Brown and A. Kodric-Brown, Ecology **58** 445, 1977.
[10] G.F. Gause, *The Struggle for Existence.* (William and Wilkins, Baltimore, 1934).
[11] C.B. Huffaker, Hilgardia **27**, 343 (1958).
[12] D. Pimentel and W.P. Nagel, Am. Nat., **97**, 141 (1963).
[13] B. Kerr, M.A. Riley, M.W. Feldman and B.J.M. Bohannan, Nature **418**, 171 (2002)
[14] B. Kerr, C. Neuhauser, B.J.M. Bohannan and A.M. Dean, *Nature* **442**, 75 (2006).
[15] M. Holyoak and S.P. Lawler, *Ecology* **77**, 1867 (1996).
[16] S. Dey and A. Joshi, Science **312**, 434 (2006).
[17] R. Durrett and S.A. Levin, Theor. Pop. Biol. **46**, 361 (1994).
[18] M.J. Keeling, H.B. Wilson and S.W. Pacala, Science 290 1758 (2000).
[19] T. Reichenbach, M. Mobilia and E. Frey, Nature **448**, 1046 (2007).

[20] E. Bettelheim, O. Agam and N.M. Shnerb, Physica **E 9**, 600 (2000).
[21] B. Cazelles, S. Bottani, and L. Stone, Proceedings of the Royal Society of London **B 268**, 2595 (2001).
[22] M. Hoyle, Ecological Modelling **202**, 441 (2007); D.B. Lindenmayer and J. Fischer, *Habitat Fragmentation and Landscape Change: An Ecological and Conservation Synthesis*. (Island Press, Washington, 2006).
[23] H. P. Possingham and I. Davies, Biological Conservation **73**, 143 (1995).
[24] A. Hastings, Ecology **74**, 1362 (1993).
[25] M. Gyllenberg, G. Söderbacka and S. Ericsson, Math Biosci **118**, 25 (1993).
[26] Y. Ben-Zion, G. Yaari and N.M. Shnerb, submitted.
[27] W.D. Hamilton and R.M. May, Nature **269**, 578 (1977); H.N. Comins, W.D. Hamilton and R.M. May, Journal of Theoretical Biology **82**, 205 (1980).
[28] More realistic models incorporate some level of "migration cost" - a finite chance of death for an individual during the migration. Here we assume no such cost. Preliminary numerical work suggests that the results presented hold, qualitatively, even if migration cost is taken into account.
[29] T. Shibata, T. Chawanya and K. Kaneko, Phys. Rev. Lett. **82**, 4424 (1999).